Hindawi Publishing Corporation
International Journal of Microwave Science and Technology
Volume 2016, Article ID 4370345, 9 pages
http://dx.doi.org/10.1155/2016/4370345

Research Article

Comparative Assessment of GaN as a Microwave Source with Si and SiC for Mixed Mode Operation at Submillimetre Wave Band of Frequency

Pranati Panda, Satya Narayan Padhi, and Gana Nath Dash

Electron Devices Group, School of Physics, Sambalpur University, Jyoti Vihar, Burla, Sambalpur, Odisha 768019, India

Correspondence should be addressed to Gana Nath Dash; gndash@ieee.org

Received 9 September 2015; Accepted 11 January 2016

Academic Editor: Salvador Sales Maicas

The potentials of GaN, SiC, and Si for application as microwave sources in mixed tunnelling avalanche transit time mode operation at submillimetre wave (sub-mm wave) frequency around 0.35 terahertz (THz) are investigated using some computer simulation methods. Design criteria to choose width, doping concentration, and area are highlighted. From the results of our simulation we observed that the Si diode produces the least power output of 41 mW followed by the GaN diode with 760 mW and the SiC diode with 2.89 W. In addition, the GaN diode has more noise than the SiC diode (by 5 dB) as well as the Si diode (by 10 dB). The drastically different performance between the GaN and the SiC diode is attributed to the incorporation of disparate carrier velocity in GaN which were not being used by other authors. In spite of the low power and high noise of the GaN compared to the SiC diode, the presence of several peaks in the mean square noise voltage curves and the existence of several minima in the noise measure curves would open a new direction in the design of GaN low-noise ATT diodes capable of multifrequency tuning like a DAR diode.

1. Introduction

The potentials of GaN for avalanche transit time (ATT) devices have been explored by several authors [1–3]. But they are based on simulation results of symmetric diode structures where the hole saturation velocity is assumed to be the same as the electron saturation velocity. This assumption is however incorrect in view of reports [4, 5]. In report [4], Albrecht et al. have used Monte Carlo simulations of electron transport based upon an analytical representation of the lowest conduction bands of bulk, wurtzite phase GaN to develop a set of transport parameters for devices with electron conduction in GaN. On the other hand, in report [5], Oğuzman et al. have calculated the hole saturation velocity using an ensemble Monte Carlo simulator, including the full details of the band structure, and numerically determined phonon scattering rate based on empirical pseudopotential method. They found that the average hole energies are significantly lower than the corresponding electron energies believed to be due to the drastic difference in curvature between the uppermost valence bands and the lowest conduction band [5]. The relatively flat valence band is responsible for hole heating, leading to low average hole energy and drastically low hole velocity compared to that for electrons. Thus there is a substantial difference in electron and hole velocities reported by the two groups. We for the first time used such disparate carrier velocities for the simulation of microwave properties of GaN MITATT (Mixed Tunnelling Avalanche Transit Time) diodes [6] and reported some interesting results from our preliminary study. The purpose of this paper is to substantiate our earlier work by extending the study and compare the results with those of the industry leader Si and the wide band gap rival SiC for operation as MITATT diodes in the same sub-mm wave band of frequency.

In avalanche transit time (ATT) diodes carrier velocities play an important role in generating the transit time phase delay which together with the avalanche phase delay produces the microwave negative resistance responsible for power production from the device. When the carrier velocities are equal, the electron and hole currents maintain the same phase leading the total current to preserve the required phase relationship with the voltage. This is the case with Si and

SiC avalanche transit time diodes where the carrier velocities are nearly equal. But such phase relationship between the *RF* voltage and *RF* current is disturbed when the electron and hole currents develop different amount of transit time phase delays from the diode active region due to disparate carrier velocities in materials like GaN. This has an adverse impact on the performance of the GaN ATT diode. We thus feel that comparing the microwave properties of the MITATT diodes based on the three materials will not only reveal their relative merits but also uncover the effect of disparate carrier velocity on the performance of the device. To start with we present the design methods for the diodes in the next section. A brief description of the simulation method is presented in Section 3 followed by results and discussion in Section 4. Finally we conclude our paper in Section 5.

2. Design Considerations

Four diode structures, three DDR (Double Drift Region) diodes based, respectively, on GaN, Si, and SiC and one SDR (single drift region) diode based on GaN, were designed for operation in sub-mm wave band at a frequency around 0.35 THz. The basic design parameters of the diode include the width, doping, and the area of cross section. The methods used to determine them are explained in the following subsections.

2.1. Width of the Active Region. For the determination of width, two criteria are generally followed. In one of them the thrust is to maximise the efficiency while the other aims at maximising the diode negative resistance. It has been seen that the efficiency is maximum when the IMPATT mode transit angle function $g_I(\theta) = (1 - \cos\theta)/\theta$ is the maximum [7]. A little amount of algebra will show that $g_I(\theta)$ will be maximum when (the appendix contains definition of symbols)

$$\theta = 2\pi f_d \tau = 0.74\pi, \tag{1}$$

where $\tau = W_{n,p}/v_{sn,sp}$ is the transit time across the diode width, f_d is the design frequency, and $v_{sn,sp}$ is the saturation drift velocity of charge carriers. With this, (1) can be manipulated to get an expression for the diode width as

$$W_{n,p} = \frac{0.37 v_{sn,sp}}{f_d}. \tag{2}$$

Now we come to the second criterion for width determination. We know that to maximise the negative resistance the phase delay between the RF voltage and RF current, θ, should be equal to π. Using this condition the expression for width becomes

$$W_{n,p} = \frac{0.5 v_{sn,sp}}{f_d}. \tag{3}$$

Once the design frequency is decided, (2) or (3) can be used to determine the required width of the diode from the knowledge of experimental values of carrier velocities for the semiconductor under consideration. Since we have chosen same frequency of operation, and since Si and SiC have equal carrier velocities, these two materials have symmetric diode structures. But, as a result of disparate carrier velocities the structures of GaN DDR diode have become asymmetric (Table 1).

2.2. Doping Concentrations. The doping profiles near the junctions can be made realistic on both donor and acceptor sides by using appropriate exponential functions. The expression used for the n-side is

$$N(x) = N_1 \left[1 - \exp\left\{\frac{x - x_j}{s}\right\}\right], \tag{4}$$

and that for the p side is

$$N(x) = N_2 \left[\exp\left\{\frac{x_j - x}{s}\right\} - 1\right]. \tag{5}$$

Here x_j is the position of the junction and N_1 and N_2 represent the flat doping levels of the n- and p-sides, respectively. In order to match the doping profiles with practical structures, the constant "s" has been taken as 5 nm. The doping profiles at the interfaces of substrate and epitaxy correspond to the solution of Fick's equation and are given by complimentary error function profiles which can be closely approximated by using exponential function of the type [8]

$$N(x) = N_H \exp\left(-1.08\lambda - 0.78\lambda^2\right), \tag{6}$$

for the n-side, and

$$N(x) = -N_H \exp\left(-1.08\lambda - 0.78\lambda^2\right), \tag{7}$$

for the p-side, where $\lambda = x''/2\sqrt{Dt}$ and x'' is the distance from the surface. The doping level, N_H, is taken to be $10^{26}/\mathrm{m}^3$ and $\sqrt{Dt}$ has been assumed to be $1\,\mu$m for our analysis. N_1 and N_2 are adjusted through several computer runs so as to maximise the efficiency and minimise the avalanche zone width. Due to the reasons described in our earlier paper [6], the doping concentration of p-side is 5 times that of n-side in the designed GaN diodes considered in this paper.

2.3. Area of Cross Section. We have used the method indicated in [9] for the determination of area of cross section of each diode structure and the same is presented in this subsection. The transit time devices such as IMPATT and MITATT diodes exhibit a negative resistance property. The admittance per unit area of such a negative resistance device is a function of the frequency and can be written as

$$Y(\omega) = G(\omega) + jB(\omega), \tag{8}$$

where $G(\omega)$ is the conductance and $B(\omega)$ the susceptance per unit area, respectively. The total diode admittance is then given by

$$\begin{aligned} Y_d(\omega) &= G_d(\omega) + jB_d(\omega) = AY(\omega) \\ &= AG(\omega) + jAB(\omega), \end{aligned} \tag{9}$$

Table 1: Design parameters of GaN DDR, GaN SDR, Si DDR, and SiC DDR diodes for operation in sub-mm wave band frequency around 0.35 THz.

Structures	Widths (nm)		Doping concentrations (10^{23} m^{-3})		Area (10^{-11} m^2)
	n-side	p-side	n-side	p-side	
GaN (DDR)	185	37	1.3	6.5	2.65
GaN (SDR)	185	—	1.3	—	0.68
Si (DDR)	117	117	3.5	3.5	2.86
SiC (DDR)	336	336	7.2	7.2	3.00

where A is the area of the device. Let us write the total diode impedance, which is the reciprocal of the diode admittance, as

$$Z_d(\omega) = \frac{1}{Y_d(\omega)} = R_d(\omega) + jX_d(\omega), \tag{10}$$

where the dynamic diode resistance can be evaluated to

$$R_d(\omega) = \frac{G(\omega)}{A\left[G^2(\omega) + B^2(\omega)\right]}, \tag{11}$$

and the dynamic diode reactance may be derived as

$$X_d(\omega) = \frac{-B(\omega)}{A\left[G^2(\omega) + B^2(\omega)\right]}. \tag{12}$$

For transit time devices at high operating frequencies it is found that $B(\omega) \gg G(\omega)$, for which (11) and (12) can be approximated, respectively, as

$$R_d(\omega) = \frac{G(\omega)}{A\left[B^2(\omega)\right]}, \tag{13}$$

$$X_d(\omega) = \frac{-1}{AB(\omega)}. \tag{14}$$

In addition to $R_d(\omega)$ the diode offers some series resistance R_S due to the finite conductivity of the semiconductor which is positive. The load offers a positive resistance R_L and a positive reactance X_L. The oscillation condition demands that $R_d(\omega) + R_S + R_L = 0$ and $X_d(\omega) + X_L = 0$. In other words $R_d(\omega)$ and $X_d(\omega)$ should both be negative which in turn implies that $G(\omega)$ is negative and $B(\omega)$ is positive. Therefore the operating frequency $\omega_p = 2\pi f_p$ is so chosen such that the device conductance has the maximum negative value while the device susceptance remains positive at that frequency; we call it the optimum frequency. For sustained oscillation therefore, we invoke (13) to obtain an expression for the diode area as

$$A = \frac{-G\left(\omega_p\right)}{\left[B^2\left(\omega_p\right)\right]\left(R_S + R_L\right)}. \tag{15}$$

The area of each diode structure has been calculated using (15). The values of peak negative conductance $G(\omega_p)$ and positive susceptance $B(\omega_p)$ are obtained from small-signal simulation described in the next section. The value of $(R_S + R_L)$ is taken to be of the order of 10 Ω. The areas of diode obtained from the calculation are input for simulation of noise program. The design parameters of all the four diode structures considered in this paper are listed in Table 1.

3. Simulation Methods

The behaviours of GaN, Si, and SiC diodes are studied by considering a one-dimensional model of diode having doping distribution of the form n^+npp^+. The microwave behaviours of the diodes are analysed for mixed mode operation. For the DC simulation we have followed the scheme described in [10]. It involves simultaneous solution of Poisson's equation, carrier continuity equation, and space charge equation. The outputs from the DC analysis are used as input for the small-signal analysis.

A small-signal method of analysis including tunnelling current to the conduction current and displacement current developed by Dash and Pati [10] is used for our study. In essence it solves two simultaneous second-order differential equations on the real and imaginary parts of the resistivity $(\rho_R(x,\omega), \rho_I(x,\omega))$ at any point x in the diode active layer, subject to the essential boundary conditions employing a double iterative computer simulation method which performs iterations over the initial values $\rho_R(0,\omega)$ and $\rho_I(0,\omega)$ since they are not known. When the iterations converge we get the final solutions $\rho_R(x,\omega)$ and $\rho_I(x,\omega)$ for a given frequency. Integrating these over the active layer of the diode one gets

$$\begin{aligned} R(\omega) &= \int_0^W \rho_R(x,\omega)\,dx, \\ X(\omega) &= \int_0^W \rho_I(x,\omega)\,dx, \end{aligned} \tag{16}$$

from where the diode conductance and diode susceptance per unit area can be obtained as

$$\begin{aligned} G(\omega) &= \frac{R(\omega)}{R^2(\omega) + X^2(\omega)}, \\ B(\omega) &= \frac{-X(\omega)}{R^2(\omega) + X^2(\omega)}. \end{aligned} \tag{17}$$

The process is repeated for several frequencies within the frequency band for which the diode is designed to determine the optimum frequency and other small-signal diode characteristics.

MITATT mode noise simulation scheme developed by Dash et al. [11] is used to analyse the noise behaviour of the designed MITATT diodes. The computation starts by putting the noise source at the beginning of the generation region. The noise electric field corresponding to the location of the

Table 2: DC and microwave properties of GaN DDR, GaN SDR, Si DDR, and SiC DDR diodes at sub-mm wave frequency band.

Material and structure	E_0 (10^8 V/m)	V_B (V)	η (%)	f_p (THz)	$G_d(\omega_p)$ (10^{-3} S)	$R_d(\omega_p)$ (Ω)	$P_{RF}(\omega_p)$ (mW)	J_T/J_0 (%)
GaN DDR	3.16	50.2	20.7	0.32	−2.415	−20.92	760	2.24
GaN SDR	3.46	44.5	21.0	0.38	−0.386	−9.97	95	6.34
Si DDR	0.757	12.2	5.89	0.30	−2.23	−9.82	41	20.45
SiC DDR	5.04	182	17.2	0.36	−0.699	−13.63	2890	18.27

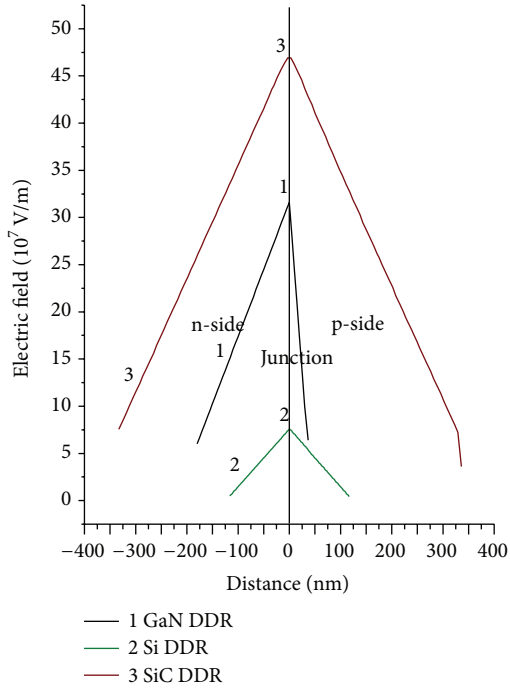

Figure 1: Electric field profiles of GaN, Si, and SiC flat doping profile DDR MITATT diodes considered in this paper.

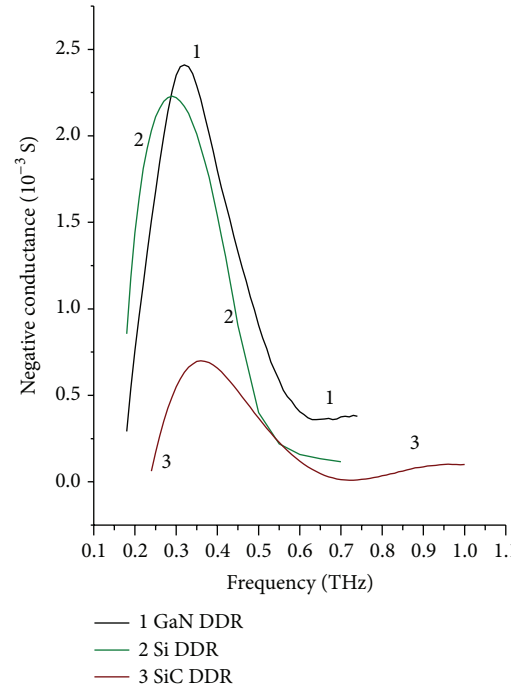

Figure 2: Negative conductance plots as a function of frequency for GaN, Si, and SiC DDR MITATT diodes referred to in Figure 1.

noise source is computed from which the terminal voltage and transfer impedances are determined. The noise source is then shifted to the next space step and the process is repeated until it covers the whole generation region. Then the mean square noise voltage and the "noise measure" (NM) are determined following the approach described in [11].

4. Results and Discussion

The DC and small-signal properties of the diodes are presented in Table 2. The design as well as the doping asymmetry of the GaN diode can be clearly seen from the table. The doping asymmetry results in not only asymmetry in the electric field profile as shown in Figure 1 but also a lower field maximum (E_0 in Table 2) for the GaN diode compared to the SiC diode. Concomitantly the SiC DDR diode has much higher breakdown voltage (V_B about 4 times) than that of the GaN diode. But, the breakdown voltage of Si DDR diode is about one-fourth of that of GaN diode. This can be understood from the fact that Si has a much lower band gap compared to SiC and GaN resulting in higher energy and higher voltage for a breakdown of the latter diodes compared to the former. Further, it can be observed from Table 2 that the GaN diode is accompanied by the highest efficiency (η), the highest negative conductance [$-G_d(\omega_p)$], and the highest negative resistance [$-R_d(\omega_p)$] at the optimum frequency (f_p). These features are indicative of superior material performance of GaN. In spite of these facts, the power output [$P_{RF}(\omega_p)$] of GaN is much less than that of SiC. The reason for such degradation in power output in GaN diode can be attributed to the disparate carrier velocities leading to lower p-side width and lower voltage drop there. This in turn decreases the breakdown voltage and hence the input voltage of the GaN diode compared to the SiC diode. Thus, although the efficiency is high, the output power is only 790 mW in the former compared to a substantial 2890 mW in the latter.

The microwave negative conductance of the device [$-G_d(\omega)$] as a function of frequency is depicted in Figure 2.

Table 3: Noise behaviours of GaN DDR, GaN SDR, Si DDR, and SiC DDR diodes at sub-mm wave frequency band.

Material & structure	f_g (THz)	$\langle v^2 \rangle / df$ (V^2s)	f_l (THz)	NM at f_l (dB)	$\langle v^2 \rangle / df$ at f_p (V^2s)	NM at f_p (dB)
GaN DDR	0.11	7.00×10^{-13}	0.35	33.50	3.97×10^{-16}	34.40
GaN SDR	0.11	3.73×10^{-12}	0.67	31.59	4.38×10^{-16}	34.23
Si DDR	0.18	2.86×10^{-14}	0.62	20.68	2.45×10^{-17}	24.59
SiC DDR	0.14	4.86×10^{-14}	0.57	25.20	1.54×10^{-16}	29.70

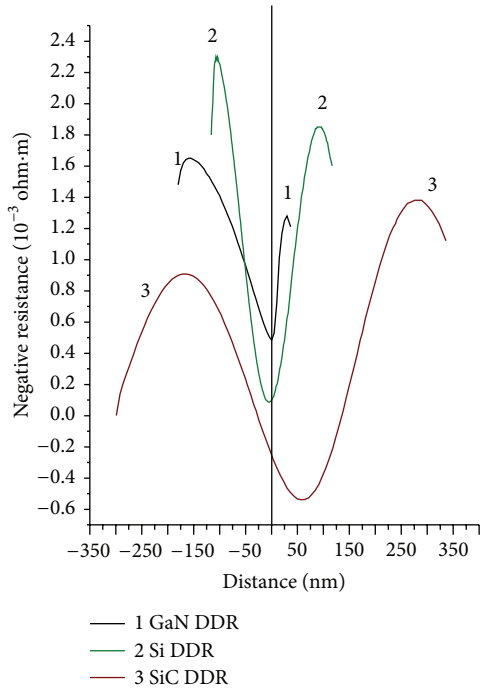

Figure 3: Negative resistivity profiles of the three DDR MITATT diodes at their respective optimum frequencies.

The GaN diode exhibits higher negative conductance compared to the Si and SiC diode over a wide range of frequencies around the design frequency of 0.35 THz. Again, the values of microwave negative resistivity as a function of distance x are computed to obtain the intensity of oscillation at each space point and to study the contribution of individual space step of the diode towards negative resistance. The microwave negative resistivity profiles $\rho_R(x, \omega_p)$ at the respective optimum frequencies are shown in Figure 3. From the figure it is observed that the $\rho_R(x, \omega_p)$ profile in each case possesses two maxima, one in each of the drift regions separated by a minimum near the diode junction. So, it is clear that the contribution to diode negative resistance mostly comes from the drift regions. The peaks in the profile of Si and SiC DDR diode are symmetrically placed with respect to the junction. But, in case of GaN DDR diode they are situated asymmetrically with the n-side peak at farther distance from the junction than the p-side peak. These features are due to equal carrier velocities in Si and SiC and inequality in carrier velocities of GaN. Further, in case of GaN and Si the magnitudes of n-side peaks are higher than that of p-side. This is because the ionisation rate of electron is higher than that for hole both for Si and for GaN. But in case of SiC the ionisation rate for holes is more than that for electrons. So for SiC diode the magnitude of p-side peak is higher than that for n-side. While the SiC diode has positive resistance contribution from the avalanche zone, the GaN diode has negative resistance contribution from the entire depletion width. This can be understood in the following way.

In SiC diode, due to equal carrier velocities, electron and hole currents develop nearly the same phase delay of π from the transit time across the diode depletion width. When combined with the avalanche phase delay of $\pi/2$ the total current, therefore, develops a phase delay of $3\pi/2$ from the drift region giving rise to negative resistance contribution from the whole of drift regions. However, due to disparate carrier velocities in GaN, the electrons develop a phase delay of π from the transit time across the diode width whereas the holes develop the same phase delay from only 1/5th of the diode width. In other words the holes will develop a phase angle of 5π as they travel across the diode width. So the hole current does not depend on the avalanche phase delay for negative resistance; the transit time phase delay is sufficient for the purpose. The diode characteristic is a manifestation of the combined phase delay of the electronic and hole currents resulting in the observed behaviour.

The percentage of tunnelling current (J_T/J_0) recorded in Table 2 reveals an important piece of information. The high tunnelling current in the Si and SiC diodes shifts the optimum frequency to a very high value around 0.8 THz due to loss in avalanche phase delay associated with the tunnelling current. In order to draw a comparative assessment, the diodes must be operated in the same frequency band (around 0.35 THz). Therefore, the widths of the Si and SiC diodes have been modulated [12] to restore the frequency to a value near the GaN diode. This makes the width of the former diodes much higher than the latter (Table 1). The noise characteristics of the diodes are presented in Table 3. It can be seen from the table that, in spite of the lower electric field in the GaN diode, it generates an order of magnitude more noise than the Si and the SiC diode as evident from the peak mean square noise voltage. From the minimum noise measure consideration also GaN diode is observed to produce 10 dB and 13 dB more noise, respectively, than SiC and Si diodes. These features are understood to be due to lower tunnelling current in the GaN diode (Table 2). The mean square noise voltage per bandwidth is plotted in Figure 4. While Si and SiC MITATT diode show single peaks in the frequency range of 0.01 THz to 1 THz, the GaN MITATT diode shows several peaks of decreasing magnitude in the same frequency range. The latter fact is indicative of the existence of several negative

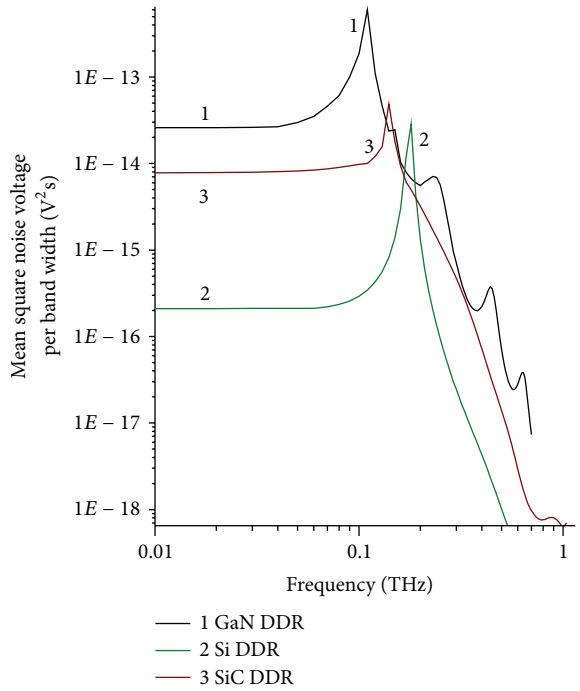

Figure 4: Mean square noise voltage per band width as a function of frequency for the three DDR MITATT diodes.

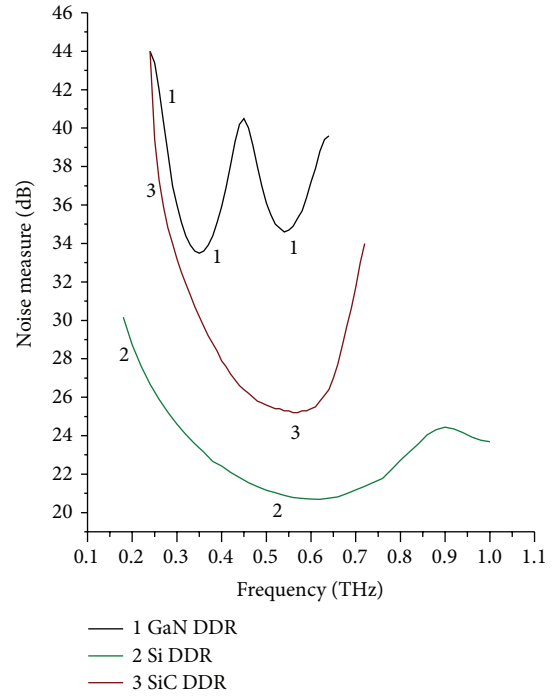

Figure 5: Noise measure characteristics of the three DDR MITATT diodes.

conductance bands in the referred frequency range. This is due to disparate phase relationship between I_n and I_p with respect to the voltage. While I_n satisfies the required phase relation for negative conductance at around 0.35 THz I_p satisfies the same at several other frequencies giving rise to multiple negative conductance bands. This is a new feature similar to that observed in a double avalanche region (DAR) diode [13]. Thus, it is believed that the GaN diode is capable of multiple frequency tuning similar to that of a DAR diode. The disparate phase relationship of the electron and hole current has the additional effect of multiple noise measure minima shown in Figure 5. This is indicative of the fact that the GaN MITATT diode has the option of being operated at more than one frequency satisfying the condition of minimum noise measure, albeit at a much higher noise level compared to the Si and SiC MITATT diodes.

An SDR structure of GaN diode has also been designed and its performance is compared with that of GaN DDR diode. The peak electric field of the SDR diode is higher than that of the DDR diode (Table 2). But, due to lower width, the SDR diode has lower breakdown voltage compared to the DDR diode. This in turn results in considerably lower power output from the SDR diode compared to that of the DDR diode. The decrease in the power output is in conformity with decrease in the value of integrated value of negative conductance (Figure 6) and negative resistance (Figure 7) of GaN SDR as compared to that of GaN DDR diode.

It is further observed from Table 3 and Figure 8 that the peak mean square noise voltage in the GaN SDR diode is almost an order higher than that in GaN DDR diode. This is because of the higher electric field in case of the former

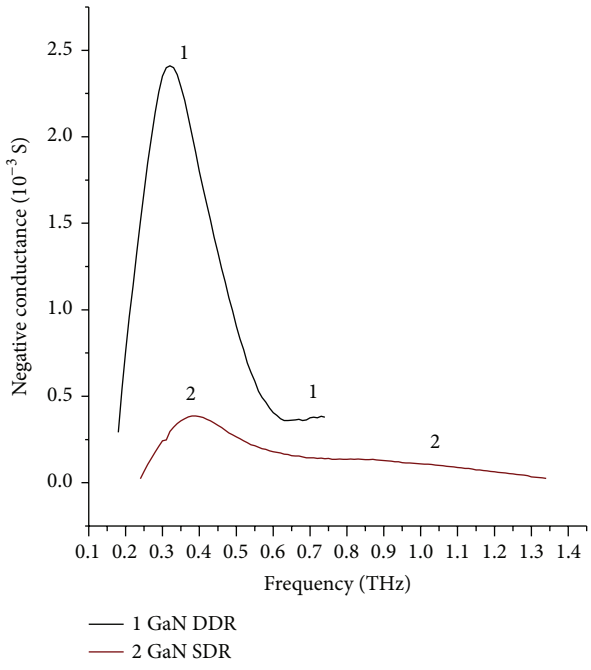

Figure 6: Negative conductance plots as a function of frequency for the GaN DDR and GaN SDR MITATT diodes considered in this paper.

than the latter. It is worthwhile noting that the percentages of tunnelling current in GaN diodes are not so high. Therefore, the effect of tunnelling current in reducing noise level has not been observed in the mean square noise voltage of diodes with this material. Further when we consider the noise measure of the DDR and SDR structures we find that it is

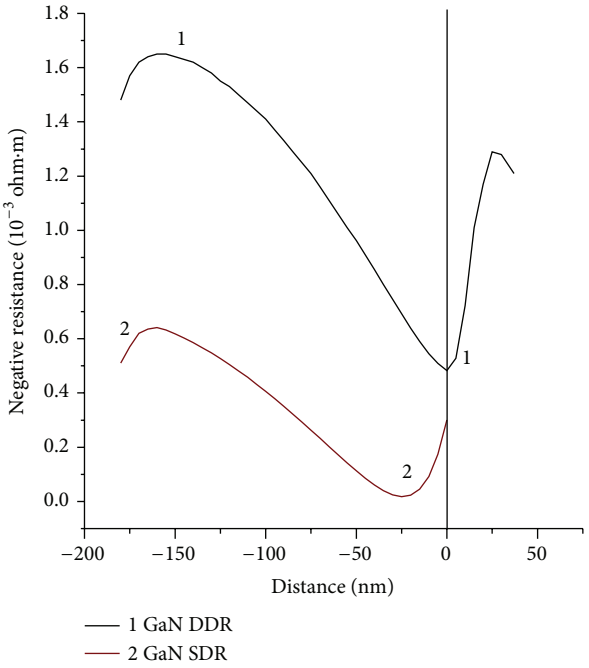

Figure 7: Negative resistivity profile of the GaN DDR and GaN SDR MITATT diodes.

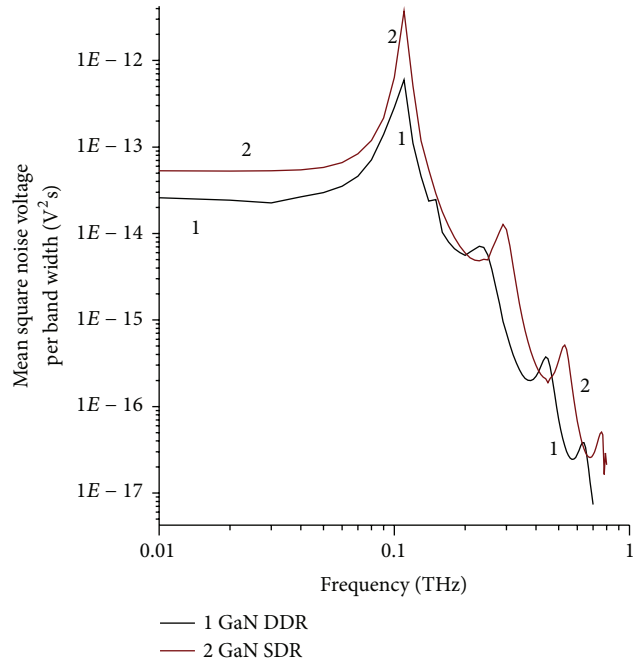

Figure 8: Mean square noise voltage per band width as a function of frequency for GaN DDR and GaN SDR MITATT diodes.

33.5 dB for the first one and 37.38 dB for the second at the operating frequency of 0.35 THz (Figure 9). Although the noise measure minimum of the SDR is 31.59 dB, which is lower than that of the DDR (33.5 dB), it is hardly of any use since it occurs at 0.67 THz where the RF properties of the diode are sufficiently degraded. Thus the effect of tunnelling current has no advantage in reducing the noise level in GaN diodes.

It is interesting to observe that the features like multiple mean square noise voltage peaks, multiple noise measure minima, and multiple negative conductance peaks observed in case of the GaN DDR diode are all present in case of the GaN SDR diode also. We consider it an additional confirmation that these features are due to the disparate carrier velocity in GaN.

5. Conclusion

The results obtained from mixed mode simulation of GaN DDR, GaN SDR, Si DDR, and SiC DDR diodes show the supremacy of GaN diodes over conventional Si diode at sub-mm wave frequency of operation in terms of both microwave power output and DC to microwave conversion efficiency. But GaN diodes are noisier than conventional Si diodes by around 13 dB with references to their minimum noise measures. Nonetheless, the microwave power output of the GaN diode is much less than that of the SiC diode. In addition, the former has 5 dB more noise than the latter at the optimum frequency. These two facts together are clear indication of the advantage of SiC over GaN for application as MITATT diode at sub-mm wave frequency. Such dismal

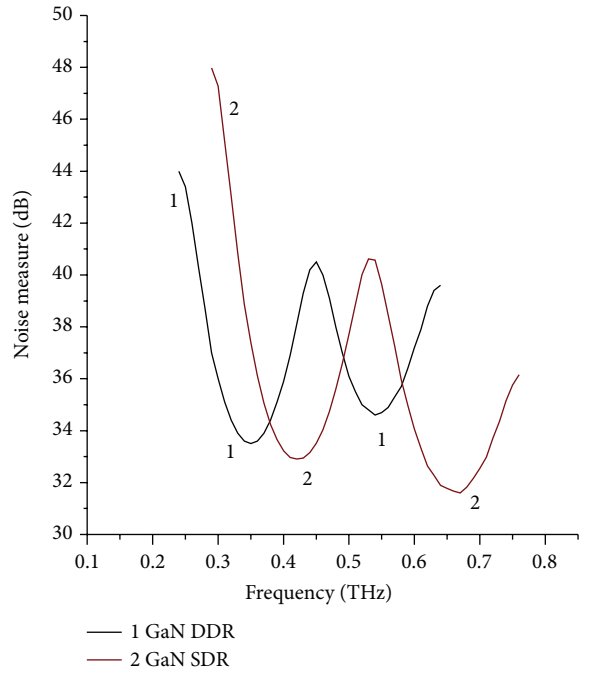

Figure 9: Noise measure characteristics of the GaN DDR and GaN SDR MITATT diodes.

performance of GaN is visibly attributable to the disparate carrier velocities. But as a silver lining in the dark cloud the disparate carrier velocities have unearthed a few interesting features of the GaN MITATT diodes. First, the presence of several peaks in the mean square noise voltage curves and the existence of several minima in the noise measure

curves would open a new direction in the design of low-noise ATT diodes. Second, the presence of several peaks in the negative conductance plots will offer the GaN diodes with a multifrequency tuning facility like that in a DAR diode.

Appendix

Definitions of Symbols

A: Area of cross section (m^2)
$B(\omega)$: Diode susceptance per unit area (Sm^{-2})
$B_d(\omega)$: Diode susceptance (S)
E_0: Peak electric field (Vm^{-1})
f_d: Design frequency (Hz)
f_g: Frequency corresponding to peak mean square noise voltage (Hz)
f_l: Frequency corresponding to minimum noise measure (Hz)
f_p: Optimum frequency, frequency at which $(-G)$ attains peak (Hz)
$G(\omega)$: Diode conductance per unit area at any frequency ω (Sm^{-2})
$G_d(\omega)$: Diode conductance at any frequency ω (S)
J_T/J_0: Ratio of tunnelling current to total current (%)
N_1: Donor doping concentration (m^{-3})
N_2: Acceptor doping concentration (m^{-3})
N_H: Doping level of substrate or epitaxy (m^{-3})
$N(x)$: Impurity doping concentration at any point x, in the diode active layer (m^{-3})
$P_{RF}(\omega)$: Power output at any frequency ω (W)
$R(\omega)$: Integrated resistivity along the diode width at any frequency ω (Ωm^2)
$R_d(\omega)$: Diode resistance at any frequency ω (Ω)
R_L: Load resistance (Ω)
R_S: Series resistance of the diode (Ω)
v_{sn}: Saturated drift velocity of electron ($m\,s^{-1}$)
v_{sp}: Saturated drift velocity of hole ($m\,s^{-1}$)
$\langle v^2\rangle/df$: Mean square noise voltage (V^2s)
V_B: Breakdown voltage of the diode (V)
W_n: Width of active layer on n-side (m)
W_p: Width of active layer on p-side (m)
x: Distance in the diode active layer (m)
x_j: Position of the junction (m)
$X(\omega)$: Integrated reactivity along the diode width at any frequency ω (Ωm^2)
$X_d(\omega)$: Diode reactance at any frequency ω (Ω)
X_L: Load reactance (Ω)
$Y(\omega)$: Diode admittance per unit area at any frequency ω (Sm^{-2})
$Y_d(\omega)$: Diode admittance at any frequency ω (S)
$Z_d(\omega)$: Diode impedance at any frequency ω (Ω)
θ: Transit angle or transit time phase delay (rad)
τ: Transit time in the drift region of the diode (s)
η: Diode efficiency (%)
$\rho_R(x,\omega)$: Real part of the diode resistivity at any space point x in the diode active layer and at frequency ω (Ωm)
$\rho_I(x,\omega)$: Imaginary part of the diode resistivity at any space point x in the diode active layer and at frequency ω (Ωm).

Conflict of Interests

The authors declare that there is no conflict of interests regarding the publication of this paper.

References

[1] S. Banerjee, M. Mukherjee, and J. P. Banerjee, "Bias current optimisation of Wurtzite-GaN DDR IMPATT diode for high power operation at THz frequencies," *International Journal of Advanced Science and Technology*, vol. 16, pp. 11–19, 2010.

[2] B. Chakrabarti, D. Ghosh, and M. Mitra, "High frequency performance of GaN based IMPATT diodes," *International Journal of Engineering Science and Technology*, vol. 3, no. 8, pp. 6153–6159, 2011.

[3] A. Acharyya and J. P. Banerjee, "Prospects of IMPATT devices based on wide bandgap semiconductors as potential terahertz sources," *Applied Nanoscience*, vol. 4, no. 1, pp. 1–14, 2014.

[4] J. D. Albrecht, R. P. Wang, P. P. Ruden, M. Farahmand, and K. F. Brennan, "Electron transport characteristics of GaN for high temperature device modeling," *Journal of Applied Physics*, vol. 83, no. 9, pp. 4777–4781, 1998.

[5] I. H. Oğuzman, J. Kolník, K. F. Brennan, R. Wang, T.-N. Fang, and P. P. Ruden, "Hole transport properties of bulk zinc–blende and wurtzite phases of GaN based on an ensemble Monte Carlo calculation including a full zone band structure," *Journal of Applied Physics*, vol. 80, no. 8, pp. 4429–4436, 1996.

[6] G. N. Dash, P. Panda, and S. N. Padhi, "Effect of disparate carrier velocity in GaN on the terahertz characteristics of double drift region mixed tunnelling avalanche transit time diode," in *Proceedings of the IEEE International Conference on Electron Devices and Solid-State Circuits (EDSSC '15)*, pp. 800–803, Singapore, June 2015.

[7] B. Culshaw, R. A. Giblin, and P. A. Blakey, "Invited paper Avalanche diode oscillators III. Design and analysis: the future," *International Journal of Electronics*, vol. 40, no. 6, pp. 521–568, 1976.

[8] V. Stupelman and F. Filaretov, *Semiconductor Devices*, Mir Publishers, 1976.

[9] G. I. Haddad and R. J. Trew, "Microwave solid-state active devices," *IEEE Transactions on Microwave Theory and Techniques*, vol. 50, no. 3, pp. 760–779, 2002.

[10] G. N. Dash and S. P. Pati, "A generalized simulation method for MITATT-mode operation and studies on the influence of tunnel current on IMPATT properties," *Semiconductor Science and Technology*, vol. 7, no. 2, pp. 222–230, 1992.

[11] G. N. Dash, J. K. Mishra, and A. K. Panda, "Noise in mixed tunneling avalanche transit time (MITATT) diodes," *Solid-State Electronics*, vol. 39, no. 10, pp. 1473–1479, 1996.

[12] G. N. Dash, "A new design approach for MITATT and TUNNETT mode devices," *Solid State Electronics*, vol. 38, no. 7, pp. 1381–1385, 1995.

[13] J. K. Mishra, G. N. Dash, and I. P. Mishra, "Simulation studies on the noise behaviour of double avalanche region diodes," *Semiconductor Science and Technology*, vol. 16, no. 11, pp. 895–901, 2001.